Physicochemical and Catalytic Properties of NiSO$_4$/CeO$_2$-ZrO$_2$ Catalyst Promoted with CeO$_2$ for Acid Catalysis

Jong Rack Sohn[*] **and Dong Cheol Shin**

Department of Applied Chemistry, Engineering College, Kyungpook National University, Daegu 702-701, Korea
[*]*E-mail: jrsohn@knu.ac.kr*
Received March 23, 2007

A solid acid catalyst, NiSO$_4$/CeO$_2$-ZrO$_2$ was prepared simply by promoting ZrO$_2$ with CeO$_2$ and supporting nickel sulfate on CeO$_2$-ZrO$_2$. The support of NiSO$_4$ on ZrO$_2$ shifted the phase transition of ZrO$_2$ from amorphous to tetragonal to higher temperatures because of the interaction between NiSO$_4$ and ZrO$_2$. The surface area of 10-NiSO$_4$/1-CeO$_2$-ZrO$_2$ promoted with CeO$_2$ and calcined at 600 °C was very high (83 m^2/g) compared to that of unpromoted 10-NiSO$_4$/ZrO$_2$ (45 m^2/g). This high surface area of 10-NiSO$_4$/1-CeO$_2$-ZrO$_2$ was due to the promoting effect of CeO$_2$ which makes zirconia a stable tetragonal phase as confirmed by XRD. The role of CeO$_2$ was to form a thermally stable solid solution with zirconia and consequently to give high surface area and acidity of the sample, and high thermal stability of the surface sulfate species. 10-NiSO$_4$/1-CeO$_2$-ZrO$_2$ containing 1 mol% CeO$_2$ and 10 wt% NiSO$_4$, and calcined at 600 °C exhibited maximum catalytic activities for both reactions, 2-propanol dehydration and cumene dealkylation.

Key Words : NiSO$_4$/CeO$_2$-ZrO$_2$, Acidity, CeO$_2$-promoting, Cumene dealkylation, 2-Propanol dehydration

Introduction

Acid catalysis is of fundamental industrial importance. It plays a vital role in many important reactions of the chemical and petroleum industries, and environmentally benign chemical processes.[1-3] The use of liquid phase superacid catalysts presents serious problems: It is difficult to separate the acid and the product stream, large amount of catalyst is usually required, and the catalyst waste is significant, causing an environmental hazard. Furthermore, the cost of process installation and maintenance is high since the liquid acids are very corrosive. It has been sought for long to replace liquid acid for solid showing comparable catalytic properties.[1] Strongly acidic sites can be created within the pores of some high silica zeolites, but, over zeolite catalysts the conversion of paraffins into branched products is low due to steric constraints. Liquid superacids based on HF, which are efficient and extensively used in catalytic processing, are not suitable for industrial processes due to separation problems tied with environmental regulations.[4] Thus the search for environmentally benign heterogeneous catalysts has driven the worldwide research of new materials as a substitute for current liquid acids and halogen-based solid acids. Among them sulfated oxides, such as sulfated zirconia, titania, and iron oxide exhibiting high thermostability, superacidic property, and high catalytic activity, have evoked increasing interest.[1,2,5] The strong acidity of zirconia-supported sulfate has attracted much attention because of its ability to catalyze many reactions such as cracking, alkylation, and isomerization.

In recent years, promoted zirconia catalysts have gained much attention for isomerization reactions due to their superacidity, non-toxicity and a high activity at low temperatures.[2,6] Sulfated zirconia incorporating Fe and Mn has been shown to be highly active for butane isomerization,

catalyzing the reaction even at room temperature.[7,8] Such promotion in activity of catalyst has been confirmed by several other research groups.[8-10] Coelho *et al*.[11] have discovered that the addition of Ni to sulfated zirconia results in an activity enhancement comparable to that caused by the addition of Fe and Mn. It has been reported by several workers that the addition of platinum to zirconia modified by sulfate ions enhances catalytic activity in the skeletal isomerization of alkanes without deactivation when the reaction is carried out in the presence of hydrogen.[12,13] The high catalytic activity and small deactivation can be explained by both the elimination of the coke by hydrogenation and hydrogenolysis, and the formation of Brönsted acid sites from H$_2$ on the catalysts.[8] Recently, it has been found that a main group element Al can also promote the catalytic activity and stability of sulfated zirconia for n-butane isomerization and ethylene dimerization.[14-16]

The search for a more active catalyst is a never ending task. At the same time that increased catalytic activity is sought, an improvement in selectivity to the desired product is also required. It is known that for zirconia-supported catalyst its surface area and catalytic activity are decreasing under the severe reaction condition such as high temperature above 600 °C.[17,18] In this paper we report new solid superacid catalyst prepared by promoting ZrO$_2$ with CeO$_2$ and supporting NiSO$_4$ on CeO$_2$-ZrO$_2$ to improve catalytic activity and thermal stability. For the acid catalysis, the 2-propanol dehydration and cumene dealkylation were used as test reactions.

Experimental Section

Catalyst Preparation. The CeO$_2$-ZrO$_2$ mixed oxide was prepared by a co-precipitation method using aqueous

ammonia as the precipitation reagent. The coprecipitate of $Ce(OH)_3$-$Zr(OH)_4$ was obtained by adding aqueous ammonia slowly into a mixed aqueous solution of cerium(III) nitrate and zirconium oxychloride (Junsei Chemical Co.) at room temperature with stirring until the pH of the mother liquor reached about 8. Catalysts containing various nickel sulfate contents were prepared by the impregnation of $Ce(OH)_3$-$Zr(OH)_4$ powder with an aqueous solution of $NiSO_4$ followed by calcining at different temperatures for 1.5 h in air. This series of catalysts is denoted by the mol percentage of CeO_2 and the weight percentage of nickel sulfate. For example, 10-$NiSO_4$/5-CeO_2-ZrO_2 indicates the catalyst containing 5 mol % of CeO_2 and 10 wt % of $NiSO_4$.

Procedure. FTIR spectra were obtained in a heatable gas cell at room temperature using a Mattson Model GL6030E spectrophotometer. The self-supporting catalyst wafers contained about 9 mg cm^{-2}. Prior to obtaining the spectra, we heated each sample under vacuum at 25-500 °C for 1 h. Catalysts were checked in order to determine the structure of the prepared catalysts by means of a Philips X'pert-APD X-ray diffractometer, employing Ni-filtered Cu K_{α} radiation. DSC measurements were performed by a PL-STA model 1500H apparatus in air; the heating rate was 5 °C per minute. For each experiment 10~15 mg of sample was used.

The specific surface area was determined by applying the BET method to the adsorption of N_2 at −196 °C. Chemisorption of ammonia was also employed as a measure of the acidity of catalysts. The amount of chemisorption was determined based on the irreversible adsorption of ammonia.[19-21]

2-Propanol dehydration was carried out at 160 and 180 °C in a pulse micro-reactor connected to a gas chromatograph. Fresh catalyst in the reactor made of 1/4 in. stainless steel was pretreated at 400 °C for 1 h in a nitrogen atmosphere. Diethyleneglycol succinate on shimalite was used as packing material of the gas chromatograph and the column temperature for analyzing the product was 150 °C. Catalytic activity for 2-propanol dehydration was represented as mol of propylene converted from 2-propanol per gram of catalyst. Cumene dealkylation was carried out at 350 and 400 °C in the same reactor as above. Packing material for the gas chromatograph was Bentone 34 on chromosorb W and column temperature was 130 °C. Catalytic activity for cumene dealkylation was represented as mol of benzene converted from cumene per gram of catalyst. The average of the first to sixth pulse values were taken as the conversions for both reactions.

Results and Discussion

Infrared Spectra. The infrared spectra of 10-$NiSO_4$/1-CeO_2-ZrO_2 (KBr disc) calcined at different temperatures (400-800 °C) are given in Figure 1. The catalyst calcined up to 700 °C showed infrared absorption bands at 1239, 1183, 1089 and 985 cm^{-1} which are assigned to bidentate sulfate ion coordinated to the metal such as Zr^{4+} or Ce^{4+}.[21,22] The band at 1625 cm^{-1} is assigned to the deformation vibration mode of the adsorbed water. For 10-$NiSO_4$/1-CeO_2-ZrO_2 calcined at 700 °C, the band intensities of sulfate ion
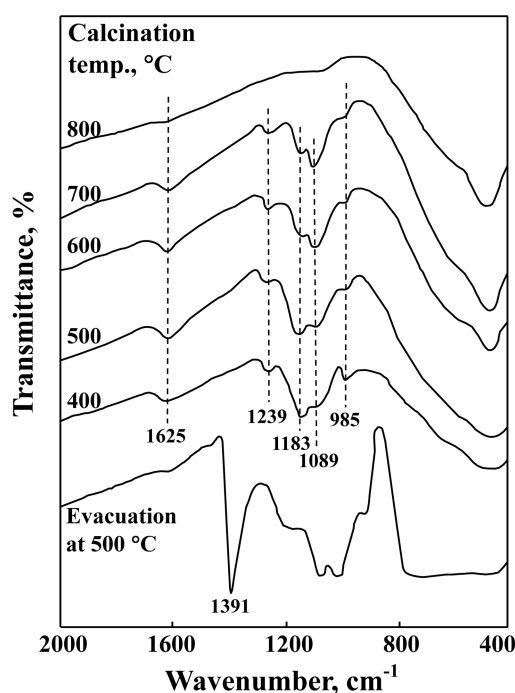

Figure 1. Infrared spectra of 10-$NiSO_4$/1-CeO_2-ZrO_2 calcined at different temperatures for 1.5 h.
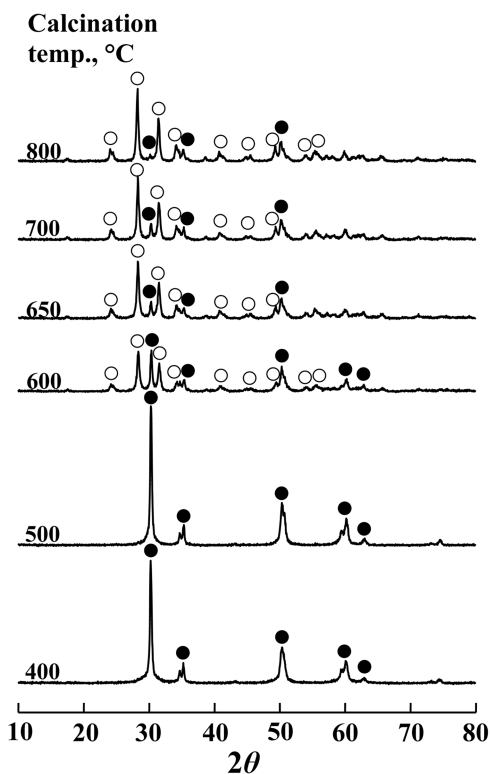
decreased because of the partial decomposition of sulfate ion. However, for the sample calcined at 800 °C infrared bands by the sulfate ion disappeared completely due to the decomposition of sulfate ion.

In general, for the metal oxides modified with sulfate ion followed by evacuation above 400 °C, a strong band assigned to S=O stretching frequency is observed at 1390-1370 cm^{-1}.[23,24] In a separate experiment infrared spectrum of self-supported 10-$NiSO_4$/1-CeO_2-ZrO_2 after evacuation at 500 °C for 1 h was examined. As shown in Figure 1, an intense band at 1391 cm^{-1} accompanied by broad and intense bands below 1250 cm^{-1} was observed due to the overlapping of the CeO_2 and ZrO_2 skeletal vibration, indicating the presence of different adsorbed species depending on the treatment conditions of the sulfated sample.[21,25]

Crystalline Structures of Catalysts. The crystalline structures of ZrO_2, 1-CeO_2-ZrO_2, and 5-CeO_2-ZrO_2 calcined in air at different temperatures for 1.5 h were examined. For pure ZrO_2, ZrO_2 was amorphous to X-ray diffraction up to 300 °C, with a two-phase mixture of the tetragonal and monoclinic forms at 400-700 °C and a monoclinic form at 800 °C (This figure is not shown here). Three crystal structures of ZrO_2, tetragonal, monoclinic and cubic phases have been reported.[26,27] However, in the case of 1-CeO_2-ZrO_2 promoted with CeO_2, the crystalline structures of the samples were different from those of pure ZrO_2. For the 1-CeO_2-ZrO_2, as shown in Figure 2, ZrO_2 was a two-phase mixture of the tetragonal and monoclinic forms at 400-600 °C and a monoclinic form at 650-800 °C. The XRD patterns of 5-CeO_2-ZrO_2 are shown in Figure 3. The crystalline structures of the samples were different from those of 1-CeO_2-ZrO_2 due to the increased CeO_2 content. As shown in Figure 3,
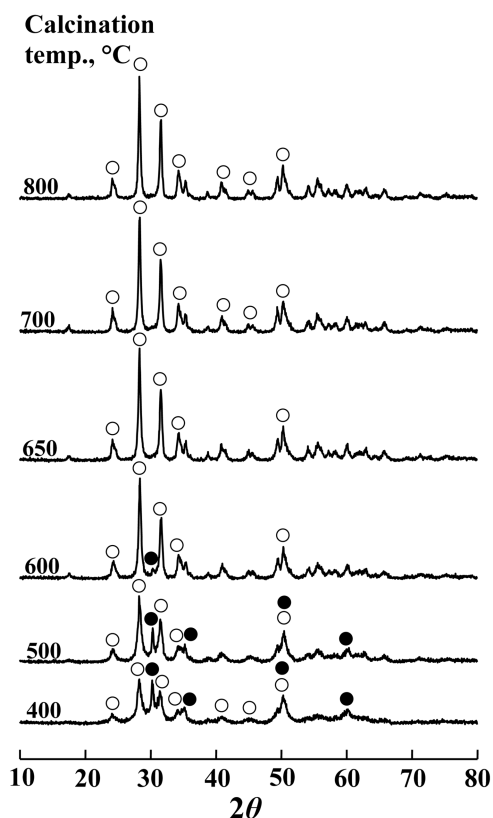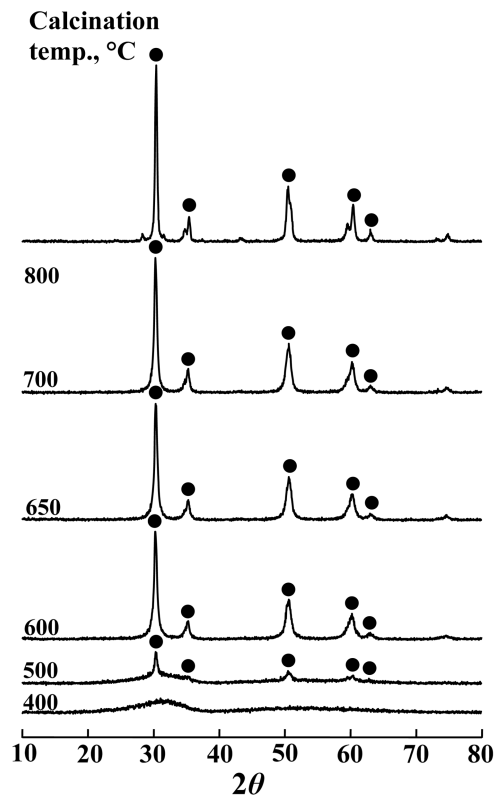
Figure 2. X-ray diffraction patterns of 1-CeO₂-ZrO₂ calcined at different temperatures for 1.5 h: (●), tetragonal phase of ZrO₂; (○), monoclinic phase of ZrO₂.

ZrO_2 was tetragonal phase up to 500 °C, with a two-phase mixture of the tetragonal and monoclinic forms at 600-800 °C. Namely, the transition temperature of ZrO_2 from tetragonal to monoclinic phase was higher by 200 °C than that of pure ZrO_2. It is assumed that the interaction between CeO_2 and ZrO_2 hinders the transition of ZrO_2 from tetragonal to monoclinic phase.[20,28] It is known that the role of CeO_2 in the catalysts is to form a thermally stable solid solution with ZrO_2.[17,18] The presence of cerium oxide strongly influences the development of textural properties with temperature.

The crystalline structures of 10-NiSO₄/1-CeO₂-ZrO₂ and 10-NiSO₄/5-CeO₂-ZrO₂ calcined in air at different temperatures for 1.5 h were checked by X-ray diffraction. In the case of supported nickel sulfate catalysts the crystalline structures of the samples were different from those of the ZrO_2, support. However, X-ray diffraction patterns of two supported catalysts are very alike because $NiSO_4$ contents for two catalysts are same and consequently they exerts the same influence on the crystalline structures of catalysts regardless of CeO_2 contents. For the 10-NiSO₄/1-CeO₂-ZrO₂ and 10-NiSO₄/5-CeO₂-ZrO₂ calcined at different temperatures, as shown in Figures 4 and 5, ZrO_2 is amorphous up to 500 °C. In other words, the transition temperature from amorphous to tetragonal phase was higher by 250 °C than that of pure ZrO_2.[17] X-ray diffraction data indicated only tetragonal phase of ZrO_2 at 600-800 °C, without detection of monoclinic ZrO_2 phase and orthorhombic $NiSO_4$ phase. However, the amount of tetragonal ZrO_2 phase increased with increasing the calcination temperature, as shown in Figures 4 and 5. It is

Figure 3. X-ray diffraction patterns of 5-CeO₂-ZrO₂ calcined at different temperatures for 1.5 h: (●), tetragonal phase of ZrO₂; (○), monoclinic phase of ZrO₂.

Figure 4. X-ray diffraction patterns of 10-NiSO₄/1-CeO₂-ZrO₂ as a function of calcination temperature: (●), tetragonal phase of ZrO₂.
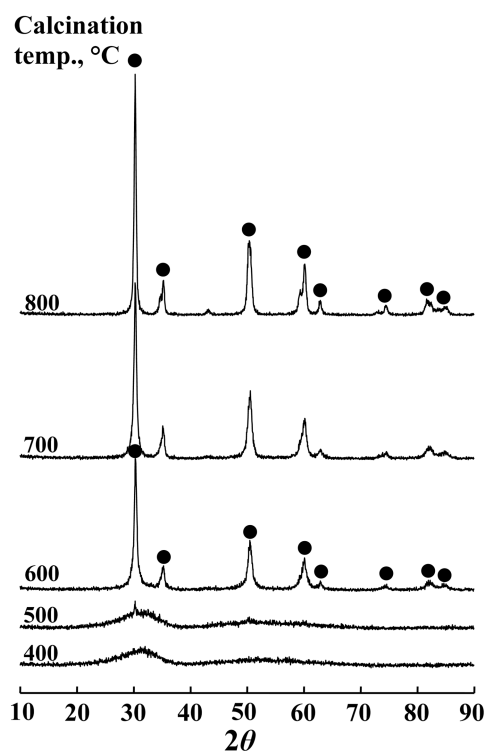
Figure 5. X-ray diffraction patterns of 10-NiSO$_4$/5-CeO$_2$-ZrO$_2$ as a function of calcination temperature: (●), tetragonal phase of ZrO$_2$.
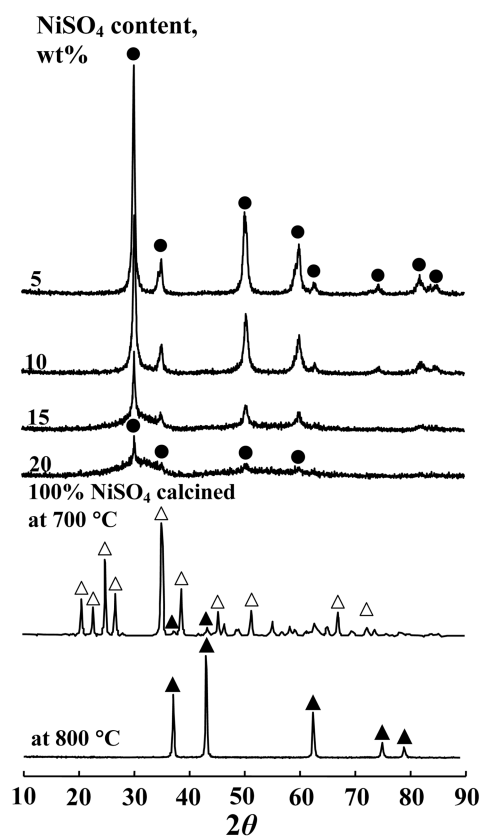

Figure 6. X-ray diffraction patterns of NiSO$_4$/5-CeO$_2$-ZrO$_2$ having different NiSO$_4$ contents and calcined 600 °C for 1.5 h: (●), tetragonal phase of ZrO$_2$; (△), orthorhombic phase of NiSO$_4$; (▲), cubic phase of NiO.

assumed that the interaction between NiSO$_4$ (or CeO$_2$) and ZrO$_2$ hinders the phase transition of ZrO$_2$ from amorphous to tetragonal.[22]

The XRD patterns of NiSO$_4$/5-CeO$_2$-ZrO$_2$ containing different nickel sulfate contents and calcined at 600 °C for 1.5 h are shown in Figure 6. XRD data indicated only tetragonal phase of ZrO$_2$ at the region of 5-20 wt % of nickel sulfate, indicating good dispersion of NiSO$_4$ on the surface of 5-CeO$_2$-ZrO$_2$. However, the higher the content of NiSO$_4$, the lower is the amount of tetragonal ZrO$_2$ phase, because the interaction between nickel sulfate and ZrO$_2$ hinders the phase transition of ZrO$_2$ from amorphous to tetragonal in proportion to the nickel sulfate content.[22] As shown in Figure 6, for pure NiSO$_4$ calcined at 700 °C, the cubic phase of NiO besides orthorhombic NiSO$_4$ phase was observed due to the decomposition of NiSO$_4$, and in the case of calcination at 800 °C only the cubic phase of NiO was observed due to the complete decomposition of NiSO$_4$ in good agreement with the result of IR in Figure 1.

Thermal Analysis. The X-ray diffraction patterns in Figures 4-6 clearly showed that the structure of NiSO$_4$/CeO$_2$-ZrO$_2$ was different depending on the calcined temperature. To examine the thermal properties of precursors of NiSO$_4$/CeO$_2$-ZrO$_2$ samples more clearly, their thermal analysis has been carried out and the results are illustrated in Figure 7. For pure ZrO$_2$, the DSC curve shows a broad endothermic peak below 200 °C due to water elimination, and a sharp exothermic peak at 418 °C due to the ZrO$_2$ crystallization.[22] However, it is of interest to see the influence of CeO$_2$ on the
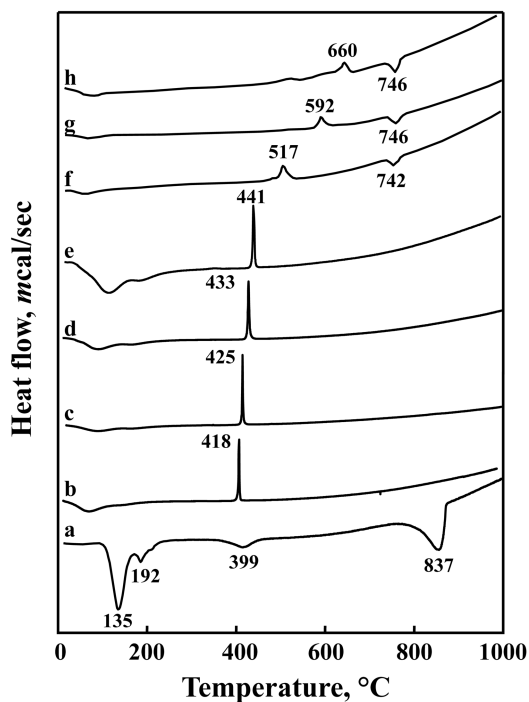
Figure 7. DSC curves of CeO$_2$-ZrO$_2$ and NiSO$_4$/CeO$_2$-ZrO$_2$ precursors having different CeO$_2$ and NiSO$_4$ contents: (a) NiSO$_4$·6H$_2$O, (b) ZrO$_2$, (c) 1-CeO$_2$-ZrO$_2$, (d) 3-CeO$_2$-ZrO$_2$, (e) 5-CeO$_2$-ZrO$_2$, (f) 5-NiSO$_4$/1-CeO$_2$-ZrO$_2$, (g) 10-NiSO$_4$/1-CeO$_2$-ZrO$_2$, (h) 15-NiSO$_4$/1-CeO$_2$-ZrO$_2$.

crystallization of ZrO_2 from amorphous to tetragonal phase. As Figure 7 shows, the exothermic peak due to the crystallization appears at 418 °C for pure ZrO_2, while for CeO_2-ZrO_2 samples it is shifted to higher temperatures due to the interaction between CeO_2 and ZrO_2. The shift increases with increasing CeO_2 content. Consequently, the exothermic peaks appear at 425 °C for 1-CeO_2-ZrO_2, 433 °C for 3-CeO_2-ZrO_2, and 441 °C for 5-CeO_2-ZrO_2.

However, for $NiSO_4$/1-CeO_2-ZrO_2 samples containing different $NiSO_4$ contents, the DSC patterns are somewhat different from those of CeO_2-ZrO_2 samples. As shown in Figure 7, the exothermic peak for $NiSO_4$/1-CeO_2-ZrO_2 due to the crystallization of ZrO_2 is shifted to more higher temperatures and the shape of peak become broad compared with that for CeO_2-ZrO_2 without $NiSO_4$, indicating that there is an interaction between $NiSO_4$ and ZrO_2 in addition to the interaction between CeO_2 and ZrO_2. These results are in good agreement with those of XRD described above. The exothermic peaks appear at 517 °C for 5-$NiSO_4$/1-CeO_2-ZrO_2, 592 °C for 10-$NiSO_4$/1-CeO_2-ZrO_2, and 660 °C for 15-$NiSO_4$/1-CeO_2-ZrO_2. The endothermic peaks for $NiSO_4$/1-CeO_2-ZrO_2 samples in the region of 742-746 °C are due to the evolution of SO_3 decomposed from sulfate species bonded to the surface of CeO_2-ZrO_2. It is reported that for sulfated ZrO_2 without CeO_2 the endothermic peak due to the evolution of SO_3 appears at 718 °C.[29] Therefore, it is clear that $NiSO_4$/CeO_2-ZrO_2 promoted with CeO_2 leads to an increase in thermal stability of the surface sulfate species due to the formation of solid solution between CeO_2 and ZrO_2. For pure $NiSO_4$·$6H_2O$, the DSC curve shows three endothermic peaks below 400 °C due to water elimination, indicating that the dehydration of $NiSO_4$·$6H_2O$ occurs in three steps. The endothermic peak around 837 °C is due to the evolution of SO_3 decomposed from nickel sulfate.[14,30] Decomposition of nickel sulfate is known to begin at 700 °C.[31]

Surface Properties

Specific surface area and acidity: The specific surface areas of samples calcined at 600 °C for 1.5 h are listed in Table 1. The presence of nickel sulfate and CeO_2 influences the surface area in comparison with the pure ZrO_2. Specific surface areas of $NiSO_4$/1-CeO_2-ZrO_2 samples are larger than that of 1-CeO_2-ZrO_2 calcined at the same temperature, showing that surface area increases gradually with increasing nickel sulfate loading up to 10 wt%. It seems likely that the interaction between nickel sulfate (or CeO_2) and ZrO_2 prevents catalysts from crystallizing.[28] The decrease of surface area for $NiSO_4$/1-CeO_2-ZrO_2 samples containing

Table 1. Surface area and acidity of $NiSO_4$/1-CeO_2-ZrO_2 catalysts containing different $NiSO_4$ contents and calcined at 600 °C for 1.5 h

| $NiSO_4$ content (mol%)	Surface area (m²/g)	Acidity (μmol/g)
0	32	40
5	67	118
10	83	184
15	40	167
20	35	136

Table 2. Surface area and acidity of 10-$NiSO_4$/CeO_2-ZrO_2 catalysts containing different CeO_2 contents and calcined at 600 °C for 1.5 h

CeO_2 content (mol%)	Surface area (m²/g)	Acidity (μmol/g)
0	45	142
0.5	79	175
1	83	184
3	77	172
5	73	169
10	44	154

$NiSO_4$ above 10 wt % is due to the block of ZrO_2 pore by the increased $NiSO_4$ loading. The acidity of catalysts calcined at 600 °C, as determined by the amount of NH_3 irreversibly adsorbed at 230 °C,[20,29,32] is also listed in Table 1. The variation of acidity runs parallel to the change of surface area. The acidity increases with increasing nickel sulfate content up to 10 wt % of $NiSO_4$. The acidity is correlated with the catalytic activity for acid catalysis discussed below.

Effect of CeO_2 addition on surface properties: We examined the effect of CeO_2 addition on the surface area and acidity of 10-$NiSO_4$/CeO_2-ZrO_2 samples. The specific surface areas and acidity of 10-$NiSO_4$/CeO_2-ZrO_2 catalysts containing different CeO_2 contents and calcined at 600 °C are listed in Table 2. Both surface area and acidity exhibited maxima upon the addition of 1 mol% CeO_2, indicating the promoting effect of CeO_2 on the catalytic activities for acid catalysis described below.

Infrared spectroscopic studies of ammonia adsorbed on solid surfaces have made it possible to distinguish between Brönsted and Lewis acid sites.[5,30,33] Figure 8 shows the infrared spectra of ammonia adsorbed on 10-$NiSO_4$/1-CeO_2-
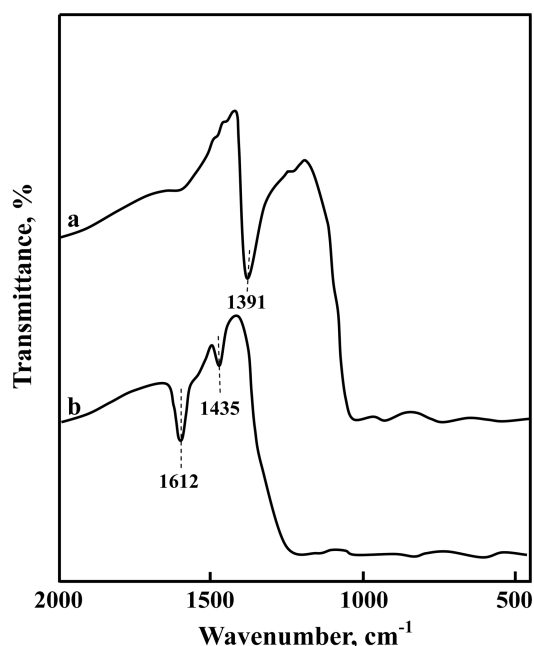
Figure 8. Infrared spectra of NH_3 adsorbed on 10-$NiSO_4$/1-CeO_2-ZrO_2: (a) background of 10-$NiSO_4$/1-CeO_2-ZrO_2 after evacuation at 500 °C for 1 h, (b) NH_3 adsorbed on (a), where gas was evacuated at 230 °C for 1 h.

ZrO_2 samples evacuated at 500 °C for 1 h. For 10-NiSO$_4$/1-CeO$_2$-ZrO$_2$ the band at 1435 cm^{-1} is the characteristic peak of ammonium ion, which is formed on the Brönsted acid sites and the absorption peak at 1612 cm^{-1} is contributed by ammonia coordinately bonded to Lewis acid sites,[5,30,33] indicating the presence of both Brönsted and Lewis acid sites on the surface of 10-NiSO$_4$/1-CeO$_2$-ZrO$_2$ sample. Other samples having different nickel sulfate contents also showed the presence of both Lewis and Brönsted acids. As Figure 8(a) shows, the intense band at 1391 cm^{-1} after evacuation at 500 °C is assigned to the asymmetric stretching vibration of S=O bonds having a high double bond nature.[24,30] However, the drastic shift of the infrared band from 1391 cm^{-1} to a lower wavenumber(not shown due to the overlaps of skeletal vibration bands of CeO$_2$-ZrO$_2$) after ammonia adsorption [Figure 6(b)] indicates a strong interaction between an adsorbed ammonia molecule and the surface complex. Namely, the surface sulfur compound in the highly acidic catalysts has a strong tendency to reduce the bond order of S=O from a highly covalent double-bond character to a lesser double-bond character when a basic ammonia molecule is adsorbed on the catalysts.[24,30]

Acids stronger than H$_o$ ≤ −11.93, which corresponds to the acid strength of 100% H$_2$SO$_4$, are superacids.[1,2,24,34] The strong ability of the sulfur complex to accommodate electrons from a basic molecule such as ammonia is a driving force to generate superacidic properties.[1,24,30] NiSO$_4$/CeO$_2$-ZrO$_2$ samples after evacuation at 500 °C for 1 h was also examined by color change method, using Hammet indicator in sulfuryl chloride.[20,35] The samples were estimated to have H$_o$ ≤ −14.5, indicating the formation of superacidic sites. Consequently, NiSO$_4$/1-CeO$_2$-ZrO$_2$ catalysts would be solid superacids, in analogy with the case of metal oxides modified with a sulfate group.[5,24,36] This superacidic property is attributable to the double bond nature of the S=O in the complex formed by the interaction between NiSO$_4$ and 1-CeO$_2$-ZrO$_2$.[2,36,37] In other words, the acid strength of NiSO$_4$/CeO$_2$-ZrO$_2$ becomes stronger by the inductive effect of S=O in the complex.
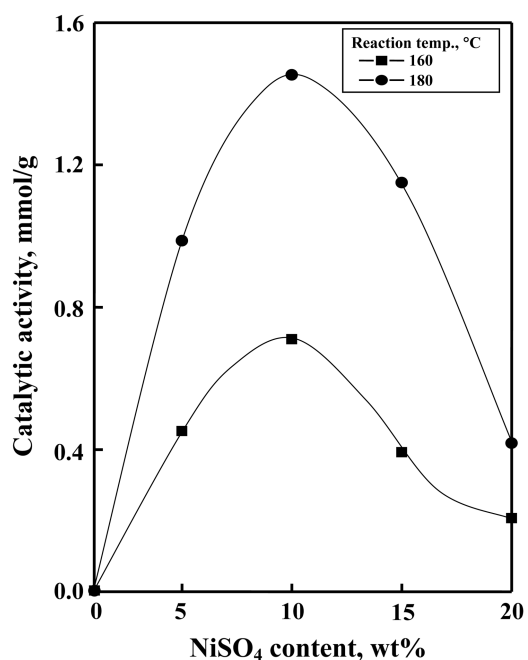
Catalytic Activities for Acid Catalysis

Catalytic activities as a function of calcination temperature: Catalytic activities of 10-NiSO$_4$/1-CeO$_2$-ZrO$_2$ for 2-propanol dehydration and cumene dealkylation are plotted as a function of calcination temperature in Figure 9. The activities for both reactions increased with the calcination temperature, reaching maxima at 600 °C, and then the activities decreased. The decrease of activities for both reactions above 600 °C can be attributed to the fact that the surface area and acidity above 600 °C decrease with the calcination temperature. Both surface area and acidity of 10-NiSO$_4$/1-CeO$_2$-ZrO$_2$ above 600 °C were found to be decreased with the calcination temperature. In fact, the surface area and acidity for 10-NiSO$_4$/1-CeO$_2$-ZrO$_2$ calcined at 600 °C were 83 m^2/g and 184 μmol/g, respectively, while those for the sample calcined at 800 °C were found to be 23 m^2/g and 30 μmol/g, respectively. Thus, hereafter, emphasis is palced only on the catalysts calcined at 600 °C.

Catalytic activities as a function of NiSO$_4$ content: It is
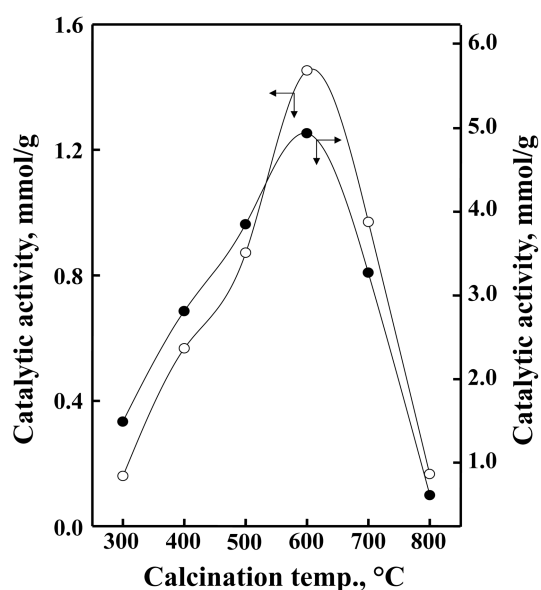
Figure 9. Catalytic activities of 10-NiSO$_4$/1-CeO$_2$-ZrO$_2$ for 2-propanol dehydration (○) and cumene dealkylation (●) as a function of calcination temperature.

Figure 10. Catalytic activities for 2-propanol dehydration as a function of NiSO$_4$ content.

interesting to examine how catalytic activity of acid catalyst depends on the acid property. The catalytic activity for the 2-propanol dehydration was measured; the results are illustrated as a function of NiSO$_4$ content in Figure 10, where the reaction temperatures are 160 and 180 °C. In view of Table 1 and Figure 10, the variation in catalytic activity for 2-propanol dehydration can be correlated with the changes of their acid amount, showing the highest activity and acidity for 10-NiSO$_4$/1-CeO$_2$-ZrO$_2$. It has been known that 2-propanol dehydration takes place very readily on weak acid sites.[5,38] Good correlations have been found in many cases

between the acidity and the catalytic activities of solid acids. For example, the rates of both the catalytic decomposition of cumene and the polymerization of propylene over SiO_2-Al_2O_3 catalysts were found to increase with increasing acid amounts at strength $H_0 \leq +3.3$.[39] It was also reported that the catalytic activity of nickel silicates in the ethylene demerization as well as in the butene isomerization was closely correlated with the acid amount of the catalyst.[30,40]

Cumene dealkylation takes place on relatively strong acid sites of the catalysts.[30,38,41] Catalytic activities for cumene
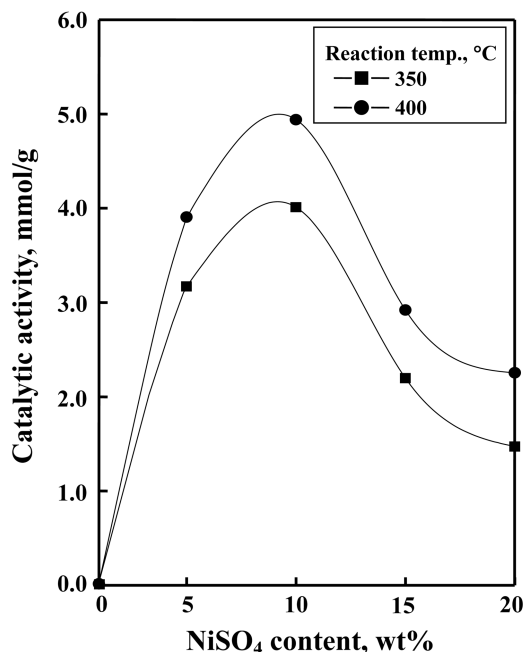

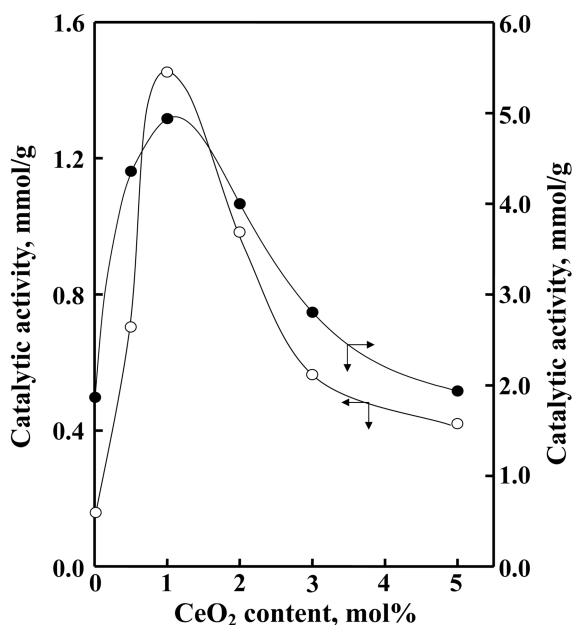**Figure 11**. Catalytic activities for cumene dealkyation as a function of $NiSO_4$ content.

Figure 12. Catalytic activities of 10-NiSO₄/CeO₂-ZrO₂ for 2-propanol dehydration (○) and cumene dealkylation (●) as a function of CeO₂ content.

dealkylation against $NiSO_4$ content are presented in Figure 11, where reaction temperatures are 350 and 400 °C. It is confirmed that the catalytic activity gives a maximum at 10 wt% of $NiSO_4$. This seems to be closely correlated to the specific surface area and acidity of catalysts. As listed in Table 1, both BET surface area and acidity attained a maximum extent when the $NiSO_4$ content in the catalyst was 10 wt% and then showed a gradual decrease with increasing $NiSO_4$ content. The correlation between catalytic activity and acidity holds for both reactions, 2-propanol dehydration and cumene dealkylation, although the acid strength required to catalyze acid reaction is different depending on the type of reactions.

Effect of CeO₂ promoting on catalytic activities: The catalytic activities of $NiSO_4$/CeO₂-ZrO₂ as a function of CeO₂ content for the reactions of 2-propanol dehydration and cumene dealkylation were examined, where reaction temperatures are 180 °C for 2-propanol dehydration and 400 °C for cumene dealkylation, respectively; the results are shown in the Figure 12. The catalytic activities for both reactions increased with increasing the CeO₂ content, reaching maxima at 1 mol%.

In general, it is known that a small amount of rare-earth solutes in nanophase zirconia powders can stabilize the tetragonal and cubic phases over a wide range of temperatures.[42] Considering the experimental results of Table 2 and Figure 12, it seems likely that the catalytic activities for both reactions closely relates to the change of acidity of catalysts. As listed in Table 2, the total acid sites of 10-NiSO₄/1-CeO₂-ZrO₂ and 10-NiSO₄/ZrO₂ are 184 μmol/g and 142 μmol/g, respectively, showing that the number of acid sites for the catalyst promoted with CeO₂ is greater than that for unpromoted catalyst. This high surface area and acidity are due to the CeO₂ promoting effect which makes
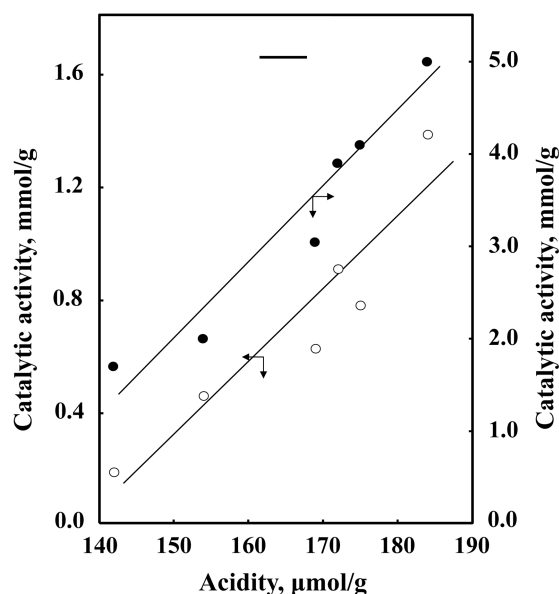

Figure 13. Correlationship between catalytic activity for acid catalysis and acidity: (○), 2-propanol dehydration; (●), cumene dealkylation.

zirconia tetragonal phase as confirmed by XRD, as shown in Figures 4 and 5. This is consistent with the results reported by Roh *et al*. over Ce-doped Ni/Ce-ZrO$_2$.[43] The promoting effect of CeO$_2$ is related to an increase in number of surface acidic sites. The catalytic activities for both reactions against acidity were illustrated in Figure 13. The correlation between catalytic activity and acidity holds for both reactions, 2-propanol dehydration and cumene dealkylation.

The formation of solid solution, CeO$_2$-ZrO$_2$ results in an increase in the thermal stability of the surface sulfate species and consequently the acidity of CeO$_2$-promoted catalyst is increased. In fact, to examine the thermal stability of the surface sulfate species DSC measurements were carried out (Figure 7). The endothermic peak due to the evolution of SO$_3$ decomposed from sulfate species bonded to the surface of ZrO$_2$ appeared at 718 ^{o}C, while that from sulfate species bonded to the surface of CeO$_2$-promoted ZrO$_2$ appeared at 742-746 ^{o}C (Figure 7). Such a temperature difference has been attributed to the stabilizing effect of the CeO$_2$ promoter on the sulfate species. The CeO$_2$-ZrO$_2$ solid solution leads to an increase in the thermal stability of the surface sulfate species and consequently the acidity of the catalysts is increased.

Conclusions

A solid acid catalyst, NiSO$_4$/CeO$_2$-ZrO$_2$ was prepared by promoting ZrO$_2$ with CeO$_2$ and supporting NiSO$_4$ on CeO$_2$-ZrO$_2$. The formation of solid solution between CeO$_2$ and ZrO$_2$ resulted in an increase in the thermal stability of the sulfate species bonded to the surface of CeO$_2$-ZrO$_2$ and consequently the acid amount and catalytic activities of catalyst were increased. The high catalytic activities of catalysts after heat-treatment at 400 ^{o}C is related to the shift of the asymmetric stretching frequency of the S=O bonds of sulfate species. The correlation between catalytic activity and acidity holds for both reactions, 2-propanol dehydration and cumene dealkylation.

References

1. Tanabe, K.; Misono, M.; Ono, Y.; Hattori, H. *New Solid Acids and Bases*; Kodansha-Elsevier: Tokyo, 1989; p 185.
2. Arata, K. *Adv. Catal.* **1990**, *37,* 165.
3. Sohn, J. R.; Lim, J. S. *Catal. Letts.* **2006**, *108*, 71.
4. Olah, G. A.; Prakash, G. K. S.; Sommer, J. *Superacids*; Wiley-Interscience: New York, U. S. A., 1985, pp 33-52.
5. Sohn, J. R.; Lee, S. H. *Appl. Catal. A: Gen.* **2004**, *266*, 89.
6. Arata, K. *Appl. Catal. A : Gen.* **1996**, *146*, 3.
7. Hsu, C. Y.; Heimbuch, C. R.; Armes, C. T.; Gates, B. C. *J. Chem. Soc., Chem. Commun.* **1992**, 1645.
8. Adeeva, V.; de Haan, H. W.; Janchen, J.; Lei, G. D.; Schunemann, V.; van de Ven, L. J. M.; Sachtler, W. M. H.; van Santen, R. A. *J. Catal.* **1995**, *151*, 364.
9. Wan, K. T.; Khouw, C. B.; Davis, M. E. *J. Catal.* **1996**, *158*, 311
10. Song, X.; Reddy, K. R.; Sayari, A. *J. Catal.* **1996**, *161*, 206.
11. Coelho, M. A.; Resasco, D. E.; Sikabwe, E. C.; White, R. L. *Catal. Lett.* **1995**, *32*, 253.
12. Ebitani, K.; Konishi, J.; Hattori, H. *J. Catal.* **1991**, *130*, 257.
13. Signoretto, M.; Pinna, F.; Strukul, G.; Chies, P.; Cerrato, G.; Ciero, S. D.; Morterra, C. *J. Catal.* **1997**, *167*, 522.
14. Hua, W.; Xia, Y.; Yue, Y.; Gao, Z. *J. Catal.* **2000**, *196*, 104.
15. Moreno, J. A.; Poncelet, G. *J. Catal.* **2001**, *203*, 153.
16. Sohn, J. R.; Cho, E. S. *Appl. Catal. A:Gen.* **2005**, *282,* 147.
17. Dong, W. S.; Roh, H. S.; Jun, K. W.; Park, S. E.; Oh, Y. S. *Appl. Catal. A: Gen.* **2002**, *226*, 63.
18. Loong, C. K.; Ozawa, M. *J. Alloys Compd.* **2000**, *303-304*, 60.
19. Sohn, J. R.; Park, W. C. *Appl. Catal. A:Gen.* **2002**, *230*, 11.
20. Sohn, J. R.; Lim, J. S. *Catal. Today* **2006**, *111*, 403.
21. Sohn, J. R.; Seo, D. H.; Lee, S. H. *J. Ind. Eng. Chem.* **2004**, *10*, 309.
22. Sohn, J. R.; Kim, J. G.; Kwon, T. D.; Park, E. H. *Langmuir* **2002**, *18*, 1666.
23. Saur, O.; Bensitel, M.; Saad, A. B. M.; Lavalley, J. C.; Tripp, C. P.; Morrow, B. A. *J. Catal.* **1986**, *99*, 104.
24. Yamaguchi, T. *Appl. Catal.* **1990**, *61*, 1.
25. Morrow, B. A.; McFarlane, R. A.; Lion, M.; Lavalley, J. C. *J. Catal.* **1987**, *107*, 232.
26. Larsen, G.; Lotero, E.; Petkovic, L. M.; Shobe, D. S. *J. Catal.* **1997**, *169*, 67.
27. Afanasiev, P.; Geantot, C.; Breysse, M.; Coudurier, G.; Vedrine, J. C. *J. Chem. Soc., Faraday Trans.* **1994**, *190*, 193.
28. Sohn, J. R. *J. Ind. Eng. Chem.* **2004**, *10*, 1.
29. Sohn, J. R.; Lee, S. H.; Lim, J. S. *Catal. Today* **2006**, *116*, 143.
30. Sohn, J. R.; Park, W. C. *Appl. Catal. A: Gen.* **2003**, *239*, 269.
31. Siriwardane, R. V.; Poston, J. A. Jr.; Fisher, E. P.; Shen, M. S.; Miltz, A. L. *Appl. Surf. Sci.* **1999**, *152*, 219.
32. Sohn, J. R.; Choi, H. D.; Shin, D. C. *Bull. Korean Chem. Soc.* **2006**, *27*, 821.
33. Satsuma, A.; Hattori, A.; Mizutani, K.; Furuta, A.; Miyamoto, A.; Hattori, T.; Murakami, Y. *J. Phys. Chem.* **1988**, *92*, 6052.
34. Olah, F. G. A.; Sommer, G. K. S. J. *Science* **1979**, *206*, 13.
35. Sohn, J. R.; Ryu, S. G. *Langmuir* **1993**, *9*, 126.
36. Jin, T.; Yamaguchi, T.; Tananbe, K. *J. Phys. Chem.* **1986**, *90*, 4794.
37. Sohn, J. R.; Park, W. C.; Kim, H. W. *J. Catal.* **2002**, *209*, 69.
38. Decanio, S. J.; Sohn, J. R.; Fritz, P. O.; Lunsford, J. H. *J. Catal.* **1986**, *101*, 132.
39. Tanabe, K. *Solid Acids and Bases*; Kodansha: Tokyo, 1970; p 103.
40. Sohn, J. R.; Ozaki, A. *J. Catal.* **1980**, *61*, 291.
41. Sohn, J. R.; Kim, J. G.; Kwon, T. D.; Park, E. H. *Langmuir* **2002**, *18*, 1666.
42. Loong, C. K.; Richardson, Jr. J. W.; Ozawa, M. *J. Catal.* **1995**, *157*, 636.
43. Roh, H. S.; Dong, W. S.; Jun, K. W.; Park, S. E. *Chem. Lett.* **2001**, 88.